System-level Simulation of Pulse Amplitude Modulation (PAM) Transmission through PMMA-POFs with Various Index Profiles

Jorge Guerrero[1,2], Dwight Richards[1], M. Angeles Losada[3], Alicia Lopez[3], Javier Mateo[3], N. Antoniades[1], Nicholas Madamopoulos[2], and Xin Jiang[1]

[1]*Department of Eng. and Env. Sci., College of Staten Island, 2800 Victory Blvd., Staten Island, NY 10314, USA*

[2]*Department of Elec. Eng., The City College of New York, 160 Convent Ave., New York, NY 10031, USA*

[3]*Photonics Tech. Group (GTF), University of Zaragoza, Mariano Esquillor Gomez, E-50018 Zaragoza, Spain*

e-mail: Jorge.Guerreroaguilar@csi.cuny.edu

ABSTRACT

In this paper, we present system-level simulation studies in PAM4 modulation using Step Index (SI) POFs, Graded Index (GI) POFs, and Multicore (MC) POFs. Our model exhibits very efficient computation time relative to models that use the finite difference method to compute the power propagation in the fiber. This makes it ideally suited for system-level investigations, where long simulation times can be quite discouraging and a real hindrance to productivity and efficiency.

Keywords: POFs, GI-POFs, Multicore POFs, Computational modeling, Optical communications.

1. INTRODUCTION

Plastic optical fibers (POFs) have a few advantages compared to glass optical fibers. Among their most important properties, stand out their physical robustness, their low-cost installation, and their tolerance to variability of lateral connector misalignment, and to localized disturbances such as bends [1]. However, the widespread adoption of POF as a transmission medium for today's increasingly high-speed applications requires a mature reliable manufacturing process. Advanced modulation formats, such as M-PAM (pulse amplitude modulation) techniques, over these multimode fibers, are also key enablers in achieving high-speed transmission [2]. Experimentally verified models can go a long way in building the confidence of a system designer.

This article aims to investigate high-speed data transmission in POF systems based on different types of POFs using our very efficient experimentally verified POF simulation models. We extend our previously reported matrix exponential method (MEM) for SI-POF [3] to both GI-POF and MC-POF. The characteristic functions (attenuation, diffusion, and mode delay) were obtained from experimental measurements to derive suitable models for each fiber type. The results reveal a high accuracy in calculating the characteristic functions (attenuation, diffusion, and mode delay) to calculate the 3 dB bandwidth and optical attenuation. We demonstrate the utility of these efficient POF models in a system-level simulation study of a PAM4 data transmission through three Polymethyl methacrylate (PMMA) POFs with 1-mm cores and different index profiles: GH4002 (SI-POF), OM-Giga (GI-POF), and SMCK-1000P (MC-POF). The first is a standard SI-POF, which typically has low bandwidth and high attenuation [4]. The OM-Giga is a PMMA fiber with a graded-index profile, which allows higher transmission rates over longer link distances, but exhibits stronger attenuation than most SI-POFs [5]. Lastly, we consider the transmission through one individual core of an MC-POF, which is composed of 19 cores arranged and consolidated inside the jacket. The main advantage of the MC-POF is its endurance against bending losses [6] and the possibility of using several cores for spatial multiplexing. The system-level simulations are conducted using the commercial simulation tool OptSim™, which allows us to easily integrate our custom POF components [7]. The results of this work demonstrate the adaptability, robustness, and precision of the computational algorithm across various POFs within a system-level framework.

2. POF SYSTEM MODELING

This section contains a concise explanation of SI-POFs, GI-POFs, and MC-POFs modeling. Guerrero et al. [3] and Stepniak et al. [8] presented an extended description of how to solve the power diffusion equation in the frequency domain in its matrix form. According to them, light propagation in POFs can be described by Equation (1):

$$\mathbb{P}_{\omega}(z=L) = \mathbb{P}_{\omega}(z=0)\ .e^{\mathbb{M}_{\omega} * L}, \tag{1}$$

where $\mathbb{P}_{\omega}(z=0)$ is the initial condition for the launching intensity distribution and the transmitted signal in the frequency domain, L is the fiber length, and $\mathbb{M}_{\omega}$ is the frequency-dependent propagation matrix, which is calculated using the characteristic functions specific for each fiber type. The vectors in Equation (1) are obtained by discretizing the angular component, θ, of the intensity spatial distributions. These frequency-dependent vectors, $\mathbb{P}_{\omega}(z)$, contain all the information to obtain fiber transmission parameters (optical power, 3 dB bandwidth, etc.).

We expanded the computational model designed for SI-POFs to encompass GI-POFs and MC-POFs, using experimental measurements for these fibers. For the SMCK, with 19 cores, we modeled the characteristic functions for these 19 cores by averaging the intensity distribution and frequency response measurements obtained for each individual core [9]. The mode group delay, $\tau(\theta)$, for SI-POFs and MC-POFs is modeled considering straight-line ray trajectories [3, 8]. For the GI-POF, we express the mode group delay, $\tau(\theta, \lambda)$, as a function of the propagation angle, θ, and the wavelength, λ, following [10]. In addition to modeling light transmission through a length of POF to simulate a typical POF link, it is necessary to model the spatial characteristics of the optical source in the transmitter, account for the effects of detector coupling, and include various components such as connectors or common disturbances such as fiber bends. Guerrero et al. [11] have a detailed explanation of the modeling of these components and effects as matrices.

Figure 1 shows the measurements in blue, magenta, and cyan and the modeled results in red, green, and yellow for OM-Giga (i.e., GI-POF), SMCK (i.e., MC-POF), and GH (i.e., SI-POF), respectively. We used the computational algorithm proposed by Guerrero et al. [3] to model the characteristic functions (attenuation, diffusion, mode delay) of the POFs. We subsequently calculated the 3 dB bandwidth and optical power output results as a function of fiber length. To quantify the accuracy of the model, we used the Normalized Mean Square Error (NMSE) to fit our model parameters to the experimentally observed data, where 1 is a perfect fit. The 3 dB bandwidth results revealed an accuracy of 0.99, 0.98, and 0.96 for the GH, SMCK, and OM-Giga, respectively. The accuracy of the optical power results is 0.96, 0.94, and 0.96 for the GH, SMCK, and OM-Giga, respectively. These results reveal the robustness, accuracy, and flexibility of the computational algorithm to model the characteristic functions for several types of POFs.

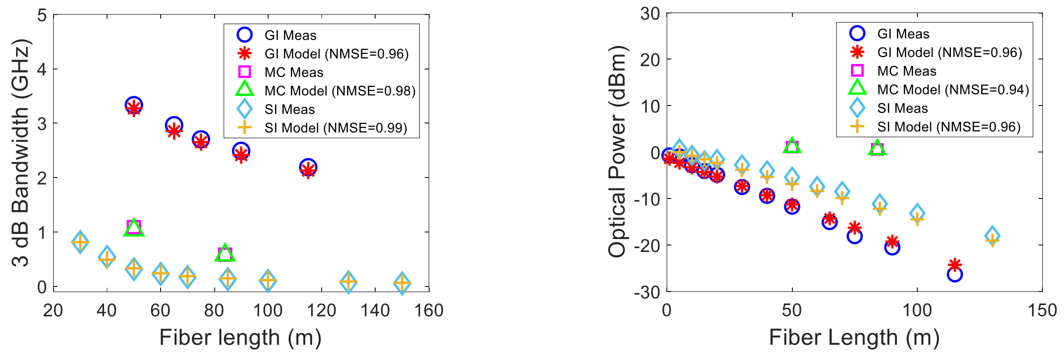

(a) *(b)*

Figure 1a. 3 dB bandwidth of GI and MC POF, (1b). Optical Power of GI and MC POF.

3. SYSTEM LEVEL MODELING

One strategy to achieve high-speed transmission over POF, although it may significantly increase the overall cost of the system, is to utilize advanced modulation schemes such as PAM4, along with DSP equalization techniques [12], which are more spectrally efficient. This section describes our reference design for a system-level study of PAM4 transmission over POFs. The ultimate objective of our work is to demonstrate that the efficient POF models that we developed for the various POF types can be utilized to rapidly assess performance at the system level.

The simulation framework is based on the OptSim™ co-simulation package using the Custom Component for MATLAB™ (CCM). This allows us to develop blocks with specific tasks in MATLAB™ and execute the system from OptSim™. The proposed CCM model, named "MEM," operated by configuring a system using the matrix model for POF and components described in the previous section. MEM functions as a subsystem in the system-level simulation, as illustrated in Figure 2(a).

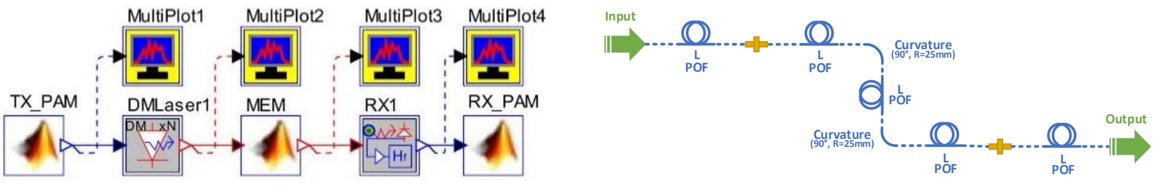

(a) *(b)*

Figure 2 (a). Topology of PAM4 transmission over POFs, (b). CCM block subsystem MEM.

Figure 2 (b) depicts the subsystem that was designed to simulate a typical POF link using the models for the three types of POFs. These segments were joined by connectors or separated by curvatures of 90 degrees with a radius of 25 mm. This subsystem is executed in MATLAB™ through OptSim™ with PAM4 modulation. We assumed a symbol rate of 1Gbd and the objective was to push to the physical boundaries of each POF type presented in this section. In order to achieve this, the fiber segments shown in Figure 2 (b) are equal lengths of each POF type, L, and the total length was noted for a predetermined bit error ratio (BER) performance. The propagation matrix that depicts the subsystem response shown in Figure 2 (b) is the following:

$$\mathbb{P}_{\omega}^{out} = M_{det} . e^{\mathbb{M}_{\omega} * L} . M_{conn} . e^{\mathbb{M}_{\omega} * L} . M_{ben} . e^{\mathbb{M}_{\omega} * L} . M_{ben} . e^{\mathbb{M}_{\omega} * L} . M_{conn} . e^{\mathbb{M}_{\omega} * L} . \mathbb{P}_{\omega}^{in}, \quad (2)$$

where $\mathbb{P}_{\omega}^{out}$ is the output intensity distribution, $\mathbb{P}_{\omega}^{in}$ is the input intensity distribution and accounts for the spatial distribution of the optical source, M_{det} is the matrix that describes the optical coupling between the POF and the detector matrix, M_{ben} is the fiber bend matrix, and M_{conn} is the connector matrix. In Figure 2 (a), this subsystem is represented by the MEM block in the middle of the OptSim™ schematic and is implemented in MATLAB™. The PAM4 transmitter and receiver are also implemented in MATLAB™ using the built-in OptSim™ DSP Library for MATLAB™. The TX_PAM model is in charge of generating an electrical PAM-4 signal with Nyquist pulse shaping and pre-emphasis. The RX_PAM model is a DSP receiver that has an embedded LMS equalization algorithm to recover the transmitted signal and estimate the BER. The complex transfer function of the CCM block subsystem is calculated from the frequency-dependent intensity distribution $\mathbb{P}_{\omega}^{out}$ obtained from Equation 2. The final output of the subsystem then becomes the product of the OptSim™ transmitter signal and the fiber transfer function, working in the frequency domain.

4. RESULTS AND DISCUSSION

This section shows the results for the 1 Gbd PAM4 transmission over the three different subsystems constituted by the three different fiber types. The results below are based on the schematic shown in Figure 2 (a). The parameters of the direct modulated laser (DMLaser1 block), such as wavelength (650 nm), relative intensity noise (-150 mdB/Hz), and threshold current (20 mA), etc., are kept constant. Additionally, the parameters of the receiver (RX1 block), such as low-pass Bessel filter and bandwidth (set at 70% of the bitrate), the quantum efficiency value (0.72), etc., are kept constant. The only change is applied in the MEM block when substituting a different fiber. In order to do a comparison of the performance of the three different fiber types, we used the simulation to estimate the cumulative sum of lengths of the equal spans of each fiber type, which allowed the system to operate below the Forward Error Correction (FEC) threshold BER of 3.7×10^{-3} [12]. Note that there are five equal spans, as shown in Figure 2 (b). For GH, SMCK, and OM-Giga the length of each fiber span is 9.6, 14, and 30.6 meters, respectively, with total fiber lengths 48, 70, and 153 meters, respectively. As an example, consider the system using the OM-Giga, Figures 3 (a) and 3 (b) illustrate the eye-diagram before and after the analog to digital conversion (ADC) and equalization, respectively. They show the effect of equalization aimed at compensating for the eye closure. The eye-diagrams for the other POFs under examination exhibit a similar behavior. Figure 3 (c) depicts the estimated BER in comparison with an ideal PAM4 reference curve. Figure 3 (d) shows a comparison of the 3 dB system bandwidth as a function of the fiber length for the three types of fiber.

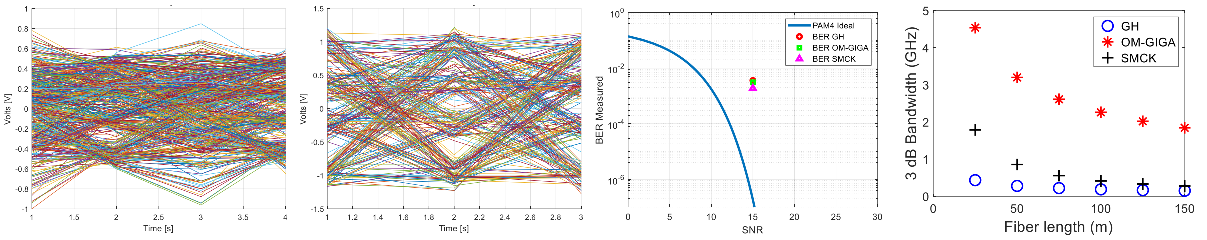

(a) (b) (c) (d)

Figure 3 (a). Pre-equalization eye-diagram of OM-Giga, (b). Output eye-diagram of OM-Giga. (c). Output BER of OM-Giga, (d). 3 dB bandwidth of the system for the three fibers.

These results reveal that the achievable lengths for GH, SMCK, and OM-Giga fibers, considering the FEC threshold BER, are 48 meters, 70 meters, and 153 meters, respectively. It is relevant to highlight that the total fiber length calculations do not include connector and bend lengths. These components introduce not only optical power loss but also changes in the intensity distribution that can alter the system frequency response. In general, our results are consistent with the physical limitations of each type of fiber. Despite MC-POFs exhibiting high resistance to bending and negligible cross-talk due to their structure (core diameter is $\sim 200\ \mu m$), the bends shown in Figure 2 (b) were modeled as standard SI-POFs, thus not accounting for the expected loss reduction. Therefore, the results of the SMCK do not fully demonstrate the potential of this type of fiber. Even though the SMCK was modeled as an individual core, it achieved 22 more meters compared to GH while maintaining a similar BER. OM-Giga exhibits the longest distance, keeping a BER similar to the other two POFs. This was expected due to its large bandwidth (> 3Gbps at 50 meters). Figure 3 (d) illustrates the 3 dB bandwidth results for the system shown in Figure 2 (a). GH exhibits the lowest bandwidth distance product, consistent with the manufacturer datasheet. SMCK reveals a better performance than GH, despite each of its cores being SI-POFs. We note that its relatively smaller core enables the transmission of fewer modes, leading to less modal delay. OM-Giga exhibits the highest bandwidth distance product. This aligns with the manufacturer's suggested bandwidth (>3 Gbps at 50 meters).

To quantify the computational time efficiency of the system shown in Figure 2 (a), we developed a system with the same topology shown in Figure 2 (a), which is based on the finite difference method. The main difference between these two methods is that the proposed computational algorithm, as shown in Equation (1), is independent of the fiber length, whereas the computational time for the finite difference method will increase drastically for longer fiber lengths. Both scenarios were executed on an Intel® Core™ i7-11800H @ 2.30GHz computer. The execution time for the GH, SMCK, and OM-Giga at lengths of 48, 70, and 153 meters was ~73 seconds each. This result is consistent with the nature of the proposed computational algorithm. In contrast, the results obtained using the finite difference method, considering a fiber length step size of 1 mm, bends, and connectors, show durations of 45 minutes and 22 seconds, 47 minutes 5 seconds, and 63 minutes 33 seconds for fiber lengths of 48, 70, and 153 meters, respectively. These results demonstrate that the scenarios based on the finite difference method require, on average, ~40 times the processing time compared to our approach. Additionally, in order to calculate the maximum fiber length for each fiber to be within the boundary of FEC, we conducted various scenarios with different fiber lengths, and the execution time remained the same (~73 seconds). If we were to conduct the same scenarios using a finite difference method system, the execution time would increase significantly. This underscores the efficiency of the proposed method in terms of the computation time.

5. CONCLUSIONS

Utilizing a system-level modeling and simulation framework is crucial for analyzing diverse POF application scenarios. The models need to be accurate, adaptable, and implement efficient computation algorithms. Our efficient POF computational algorithm and system simulation methodology demonstrate promising accuracy, and computational processing time (~73 seconds, 40 times less than the standard calculations). Now, our method encompasses models for POFs of different index profiles and for several components (connectors and curvatures) and various modulation formats. The overarching goal is to enable POF system-level simulations that depict realistic scenarios, enabling cost and resource savings by accurately predicting system behavior before the deployment of physical systems. As existing and new applications, primarily driven by artificial intelligence (AI), demand more and more data, we anticipate the need to transmit high-speed data over various POF types. Our PAM4 simulation example demonstrates that this is feasible and also that our system-level simulation approach can help accelerate the research efforts in this niche application area.

ACKNOWLEDGEMENTS

This work has been sponsored by the National Science Foundation (NSF) under GOALI grant 1809242, by Gobierno de Aragon (DGA) under grant T20-23R, and by MICINN/FEDER under grants RTI2018-094669-B-C33 and PID2021-122505OB-C33. The APC was funded by the NSF. The authors would like to thank Synopsys Inc. for providing OptSim™ as part of their University Software Program.

REFERENCES

[1] O. Ziemann *et al.*: POF Handbook, 2nd ed. (Springer, 2008).

[2] G. Stepniak *et al.*: Polymer-optical-fibres-for-data-transmission, Chapter 8 in Polymer Optical Fibres Fibre Types, Materials, Fabrication, Characterisation, and Applications, 1st ed., Elsevier, The Netherlands, 2017.

[3] J. Guerrero *et al.*: Novel Measurement-Based Efficient Computational Approach to Modeling Optical Power Transmission in Step-Index Polymer Optical Fiber, *Photonics 2022*, 9, 260.

[4] M.A. Losada *et al.*: Experimental Assessment of the Transmission Performance of Step Index Polymer Optical Fibers Using a Green Laser Diode. *Polymers 2021*, 13, 3397.

[5] A. Lopez *et al*.: Experimental Characterization of the Transmission Properties of Large-Core Graded-Index PMMA Fibers, *in Proc. Of the 22nd International Conf. on Transparent Optical Networks (ICTON 2020).*

[6] S. Sasho: A Comprehensive Bending Loss Study of Multi-core POF, *in Proc. Int. Conf. Plastic Optical Fibers*, Santa Clara (U.S.A.), 2008.

[7] D. Richards *et al.*: Overcoming challenges in large-core SI-POF-based system-level modeling and simulation, *Photonics 2019*, 6(3), 88.

[8] G. Stepniak *et al.*: Modeling of transmission characteristics in step-index polymer optical fiber using the matrix exponential method, *Applied Optics*, vol. 57, issue 31, pp. 9203-9207 (2018).

[9] Seron *et al.*: Experimental Characterization of the Transmission Properties of Individual Cores in PMMA Multicore, *POF 2022*, Bilbao, Spain (2022).

[10] A. Simović *et al.*: Investigation of bandwidth in multimode graded-index plastic optical fibers, *Opt. Express 29*, 29587-29594 (2021).

[11] J. Guerrero *et al.*: Modeling and simulation of large-core SI-POF and GI-POF based on a system-level framework, *POF 2022*, Bilbao, Spain (2022).

[12] A. Yekani *et al.*: Experimental comparison of PAM vs. DMT using an O-band silicon photonic modulator at different propagation distances, *2015 European Conference on Optical Communication*, 2015.